Environ. Sci. Technol. **2000**, *34,* 3540−3546

The Diversity of Natural Hydrous Iron Oxides

DIDIER PERRET,*,† JEAN-FRANÇOIS GAILLARD,‡ JANUSZ DOMINIK,§ AND OLIVIER ATTEIA||,#

Institut de Chimie Minérale et Analytique, Université de Lausanne, CH-1015 Lausanne, Switzerland, Department of Civil Engineering, Northwestern University, Evanston, Illinois 60208-3109, Institut F.-A. Forel, Université de Genève, CH-1290 Versoix, Switzerland, and Centre d'Hydrogéologie, Université de Neuchâtel, CH-2007 Neuchâtel, Switzerland

Three different aquatic environments (one deep meromictic lake, Lake Lugano, CH; one shallow meromictic lake, Paul Lake, U.S.A.; and one peat-land crossed by a river, Vallée des Ponts, CH) were studied. The physicochemical characteristics of hydrous iron oxides identified in these systems were determined by spatially resolved analytical electron microscopy at the level of individual submicrometric particles. High molecular weight natural organic matter, dominantly polysaccharides (lakes) or humics (peat-land), serves as a template for the formation and growth of these particles and governs their final morphology. Depending on the waters, networked microgranules, ill-defined entities, or quasi-spherical globules were identified. These Fe−C-rich particles also contain large proportions of other elements (*e.g.*, P, Ca, Si); they are thus fundamentally different from pure synthetic iron oxides used in the laboratory to infer their transport and sorptive properties. We show that the morphotypes of aquatic iron oxides are influenced by the combined effect of basic environmental parameters, *e.g.*, the ionic strength, the relative concentrations of total iron and organic matter, the nature of the organic matter, and to a lesser extent the pH in the waters.

Introduction

In aquatic systems, hydrous iron oxide particles have been recognized for decades as ubiquitous carriers of trace elements, i.e., nutrients *(1, 2)*, metals *(3−7)*, and organic contaminants (*8, 9*). In most instances, only the total concentration of particulate iron is determined following some operationally defined schemes such as filtration *(10)*. Such measurements provide only averaged chemical information of the bulk water sample that mask the detailed nature of individual particles. Then, the prediction of sorptive properties of this particulate material relies primarily on surface speciation models, calibrated in the laboratory using well characterized iron oxides *(11)*, and based on thermodynamic considerations and conceptual views of the surface-water interface *(7, 12, 13)*.

However, these synthetic phases usually bear little resemblance to natural particles, as we shall demonstrate here. Hence, it becomes evident that an accurate description of the transport pathways and the reactivity of these aquatic particles require more information at the microscopic level. The knowledge of the physical and chemical characteristics of iron-rich suspended matter, at the scale of individual particles, is thus compulsory to understand and predict the role that iron oxides play in the fate of contaminants in natural waters. In this study, we present microscopic observations of the morphology, elemental composition, and evolution of iron-rich particles in several aquatic environments to stress that conventional notions about iron-organic interactions need to be revised.

Hydrous iron oxide particles are produced at oxic-anoxic interfaces in soils, sediments and natural waters *(14, 15)*. They are generally depicted as poorly crystallized globules *(16−20)*. On one hand, it has been shown that low to medium molecular weight natural organic matter (NOM) coats the surface of these particles, affecting their surface charge and adsorption behavior *(21)*. On the other hand, poorly characterized macromolecular natural organic matter (MNOM), of living or nonliving origin, is usually not taken into account in the genesis of hydrous iron oxides *(17, 18)*. However, interactions between colloidal organic matter and iron-rich globules may lead to bridged entities with modified coagulation/sedimentation properties *(22)*. In addition, organic matter may catalyze and accelerate electron transfers during oxidation of Fe(II) by oxygen, leading to blended organic-iron particles with specific surface reactivities, or increase the stability of Fe(III)-NOM complexes, resulting in a reduced Fe(III)/Fe(II) redox potential *(23, 24)*. Last, the inclusion of foreign ions into the iron phase during particle formation may modify their reactivity *(25)*.

Although the literature on the characterization and role of iron oxides in natural waters is abundant, there has been no clear attempt to link their final morphology to the physicochemical parameters of the waters where their genesis takes place. The purpose of this paper is to investigate the morphotypes and the elemental compositions of hydrous iron oxides formed in various natural settings by using direct observation techniques, i.e., transmission electron microscopy. We selected three different sites, a large eutrophic and meromitic lake, a small meromictic lake, and a peat-land that present diverse physicochemical characteristics, and therefore offer a unique opportunity to probe individual Fe-rich particles under real natural conditions. Instead of focusing on the results of the three specific sites, we propose to generalize our observations and to use the basic physicochemical parameters of water bodies as key parameters to infer the final characteristics of hydrous iron oxides.

Materials and Methods

Water samples were collected from the oxic/anoxic transitions that develop in two meromictic lakes; the Lake Lugano (Ticino, Switzerland) *(26, 27)* and Paul Lake (MI) *(27, 28)*. In addition, a third set of samples was obtained from the peat-land of the Bied River (Neuchâtel, Switzerland) *(29, 30)*. Lake Lugano is located by 46°00′N−9°00′E. It is a large eutrophic and meromictic lake that has three interconnected basins. The north basin, the Gandria basin where the study was conducted, has a surface area of 27.5 km^2 and a maximum depth of 288 m. The oxycline lies at a depth of about 80 m. The concentrations of major ions, present in Lake Lugano

* Corresponding author phone: +4121-6923923; fax: +4121-6923935; e-mail: didier.perret@icma.unil.ch.

† Université de Lausanne.

‡ Northwestern University.

§ Université de Genève.

|| Université de Neuchâtel.

Present address: Institut EGID, Université Bordeaux III, F-33405 Talence, France.

10.1021/es0000089 CCC: $19.00
Published on Web 07/26/2000

surface waters, reflect the predominance of carbonated rocks, i.e., calcite and dolomite, and gypsum in the catchment. In contrast, Paul Lake (MI), located by 46°13′N−89°32′W, is a small (surface area of 1 ha, and a maximum depth of 13 m) mesotrophic kettle lake characterized by a biogenic meromixis and a low mineralization, i.e., the conductivity of surface waters is about 12 μS. The depth of the oxic/anoxic transition varies between 5 and 7 m. The third aquatic environment is the peat-land of the Bied River at the Vallée des Ponts. It is located by 47°01′N−6°50′E and has a surface area of 60 km^2. The valley is covered by peat and crossed by the Bied River. The pore waters are circulating through the peat and are collected by drains that are directly connected to the river.

Water samples were collected at all these locations by peristaltic pumping and were retrieved, in line, using 50 mL syringes or tubes, which were immediately sealed, transferred to a N_2-purged glovebag (model X27−27, I^{2}R), and brought back to a laboratory. Specimen grids (200 mesh, Cu, carbon-coated and collodion-covered, SPI Supplies) for transmission electron microscopy (TEM) were placed at the bottom of Nalgene centrifuge tubes. Under N_2 atmosphere, an aliquot of the bulk water sample was transferred to centrifuge tubes (30 mL) that were tightly sealed. The volume of aliquot used was determined from turbidity measurements in order to ensure appropriate final particle coverage on the grid. The tubes were spun, usually under nitrogen atmosphere, within 30 min to 2 h after retrieval from the field using a swing-out rotor to obtain whole mount specimens. After centrifugation, the tubes were transferred to a glovebag, and the supernatant was carefully withdrawn, by slow nonturbulent removal using cleaned pipets. In most instances, the TEM grids were then protected with a thin film of hydrophilic resin (Nanoplast FB101; Plano). Previous laboratory tests showed that, under these conditions, Fe(II) is not oxidized into Fe(III)part. More details about this sampling procedure are presented elsewhere *(31, 32)*.

In addition, ancillary measurements such as depth profiles (for lakes) or subsurface profiles (for the peat-land river site) of temperature, pH, dissolved oxygen, dissolved and particulate iron, manganese, silicon, aluminum, calcium, magnesium and phosphate were performed using methods that have been detailed in previous papers *(31, 33−35)*. Briefly, continuous depth profiles were recorded using either an Zullig Hydropolytester-D probe (Lugano) or an Hydrolab Minisonde (Paul). Total iron was analyzed either by atomic emission spectrometry (ICP-AES) after acidification of whole water samples with nitric acid or by colorimetry after reacting the samples with hydroxylamine hydrochloride and Ferrozine assay. After filtration of whole water samples through 0.45 μm pore size filters, dissolved Fe was measured either by atomic emission spectrometry (ICP-AES) or as Fe(II) by colorimetry using Ferrozine. Particulate Fe was determined by difference between total Fe and dissolved Fe. Dissolved and total manganese, silicon, aluminum and calcium were determined by graphite furnace or flame atomic absorption (GFAAS, FAAS) or by ICP-AES. Total organic carbon (TOC) was measured by high-temperature catalytic oxidation using a Shimadzu TOC-5000. Last, phosphates were determined by colorimetry, using the molybdenum blue method.

TEM identifications were then performed on a medium-resolution TEM Zeiss EM10 (80 keV, nominal magnification: 10000−80000×; Centre de Microscopie Electronique, University of Lausanne), while elemental microanalyses were performed on High-Resolution Electron Microscopes: either a Philips CM12 (80 keV, 10000−150000×, Centre de Microscopie Electronique) equipped with an EDAX-STUV windowless detector or an Hitachi HF-2000 FEG (200 keV, 70000−400000×, Centre Interdépartemental de Microscopie Electronique, EPFL, Lausanne) equipped with a Noran Ge/Norvar detector. These instruments are equipped with narrow probes (CM12: ca. 40 nm; HF-2000: ca. 2 nm in diameter) that provide X-ray spectrometry (energy dispersive spectrometry, EDS) with a high lateral definition. The beam sampling depth was estimated to equal the thickness of the analyzed particles under the conditions of operation.

Results and Discussion

Figures 1−3 present composite pictures showing the water chemistry, typical iron oxide morphology, and nanoscale elemental EDS spectra obtained from these oxides at the three locations. Water profiles across the oxic/anoxic transition are presented for the two lakes, whereas for the peat-land, selected sampling sites characterized by increasing amounts of oxygen are shown. Several additional parameters describing the physicochemical characteristics of the waters are discussed below; their profiles are detailed elsewhere *(26−31, 33−35)*.

In lake Lugano (Figure 1), the oxycline extends over more than 20 m and is followed by a well-defined peak of particulate iron that occurs about 12 m below the complete depletion of oxygen. Across this transition, the TOC concentration remains quite featureless and the pH smoothly decreases from 7.6 to 7.4 with depth, whereas the concentration of ΣPO_4 smoothly increases downward from 0.5 μM up to 10 μM, while the maximum of $[Fe]_{tot}$ reaches 7 μM just above the sediment. In addition, a 25 m thick layer of Mn_{part} can be identified above the Fe_{part}-rich layer, and ΣH_2S appears below the peak of Fe_{part} and reaches 15 μM just above the sediment. The shape of these profiles is observed throughout the year.

The micrograph in Figure 1 shows a typical iron-rich particle collected in the peak of particulate iron. The EDS spectrum obtained after focusing of the electron beam at the granule indicated by the arrow is displayed below the micrograph. The complete set of iron-rich particles analyzed by TEM-EDS (n = 1096 entities) exhibits the same morphological and compositional features, whatever the depth within the peak of Fe_{part} or the sampling period (11 sets of samples collected between Spring and Summer 1996, for $z_{sampling}$ = 85−120 m).

In Paul Lake (Figure 2), the same chemical parameters are presented. In this case however, the oxic/anoxic transition spans only just over one meter. There is a net increase in the TOC content with depth. As opposed to Lake Lugano, the optimal photosynthetic activity is observed close to the surface, within the 3−6 m layer, where the pH is optimum (ca. 7.0), prior to its decrease in the zone of oxygen consumption to reach 6.4−6.5 below the peak of iron-rich particles *(31)*. In contrast, the peak concentration of particulate iron is quite pronounced compared to the previous case, i.e., 0.28 μM for Lake Lugano vs 110 μM for Paul Lake. Across this thin redox transition in Paul Lake, the concentration of ΣPO_4 increases sharply from below detection limits to 0.3 μM below the peak of Fe_{part}; a 1.5 m thick layer of Mn_{part} is identified just above the Fe_{part}-rich layer; and sulfides appear at 8 m to reach ΣH_2S = 15 μM just above the sediment, where the concentration of dissolved iron reaches 150 μM. Here again, the profiles shown are representative of the situation encountered throughout the year in this lake characterized by a biogenic meromixis, with however some slight variations from year to year.

As before, a micrograph of a typical iron oxide particle is shown together with the associated EDS spectrum. In the case of Paul Lake, ca. 200 iron-rich particles collected between 6 and 10 m were analyzed by TEM-EDS, during the summers of 1995 and 1996; they systematically exhibited features similar to the ones shown in Figure 2.

In the Bied River (Figure 3), the pH, the concentrations of O_2 and Ca^{2+}, and the conductivity increase from peat to river, while the ratio $[Fe(II)]/[Fe]_{tot}$ simultaneously decreases.

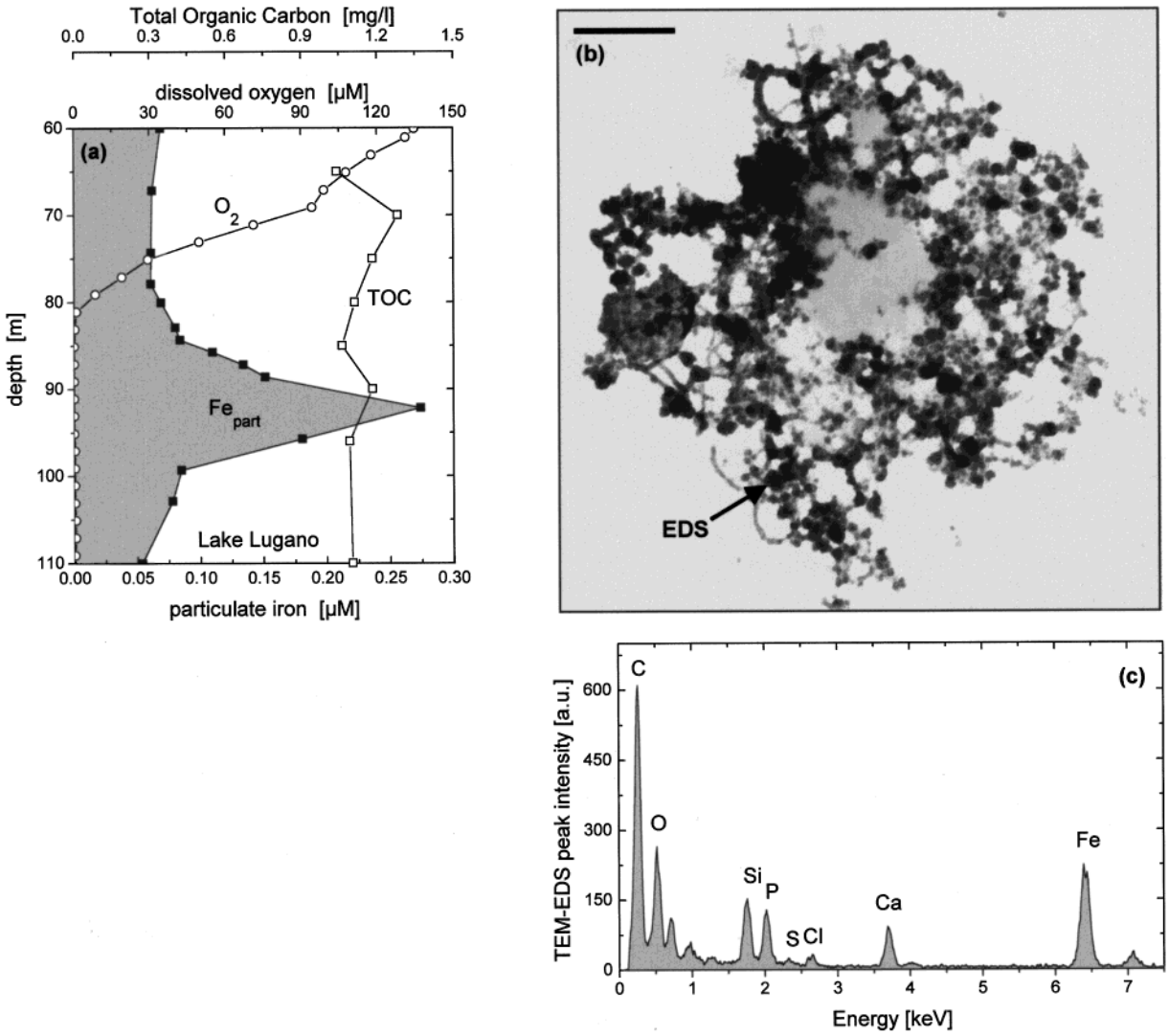

FIGURE 1. (a) Concentration profiles of $[O_2]$, $[Fe]_{part}$ and TOC in the water column of Lake Lugano. (b) Transmission electron micrograph (TEM) of typical Fe-rich entities sampled at the maximum of the peak of Fe_{part} (scale bar = 500 nm). (c) Typical elemental analysis (TEM-EDS) of an assemblage of Fe-rich entities connected together on a network of fibrillar polysaccharides.

The increases in pH and in the concentrations of Ca^{2+}, Al, and Si result from the weathering of the subsurface carbonated clay stratum. Correlated UV (285 nm) vs TOC measurements throughout the valley indicates that NOM is mainly of humic/fulvic origin. The concentrations shown in Figure 3 are representative of the usual low water flows measured in the river.

Micrographs of iron-rich particles in the river demonstrate relatively consistent shapes and a strong morphological similarity with carbon-rich particles identified in the peat pore water. Iron-rich particles such as the ones shown in Figure 3 predominate the pool of particles in the drains and in the river (ca. 1200 particles analyzed between 1995 and 1998).

All of our microscopic observations show that macromolecular natural organic matter, MNOM, is systematically involved in the production and trapping of hydrous iron oxides. It is remarkable that transmission electron micrographs of specimens obtained under nondisturbing conditions *(32, 36)* from the Fe-rich layers of Lake Lugano (Figure 1b), Paul Lake (Figure 2b) and from the Bied River (Figure 3d) systematically reveal particles with very different morphologies. Elemental analyses (by energy dispersive spectrometry, Figures 1c, 2c, 3g) confirmed that these particles contain a dominant proportion of iron but that their intimate composition differs from site to site. Note that in these spectra, the peaks of carbon and oxygen are not representative of the particles analyzed, because the latter are deposited on a carbon-collodion supporting film.

In Lake Lugano, miniature granules (diameter ca. 10−50 nm) are always embedded in networks of fibrillar organic matter connected to their parent bacteria. In Paul Lake, large scale interconnected organic fibrils are rendered electron-dense by a natural iron stain and always form a material that is morphologically ill-defined. In the Bied River, large (100−500 nm) particles always appear as either spheres or asymmetric drop-like globules. At each site, Fe-rich particles contain nonnegligible amounts of P (Lugano: P:Fe $\approx$ 0.5), Ca (Bied: Ca:Fe $\approx$ 0.4) or Si (Paul: Si:Fe $\approx$ 0.2), and other elements (Al, S, Cl).

In both lakes, photosynthetic activity leads to the production of aquagenic organic matter, such as extracellular polymeric substances, EPS. The omnipresence of lacustrine EPS was unequivocally assessed by TEM with a highly selective stain generating nanometer-sized silver grains on neutral/acidic polysaccharides *(34, 37, 38)*. TEM examination of Ag-labeled specimens revealed polysaccharides ranging from large fibers to ultrathin (<5 nm) networked fibrils, confirming the dominant aquagenic origin of lacustrine

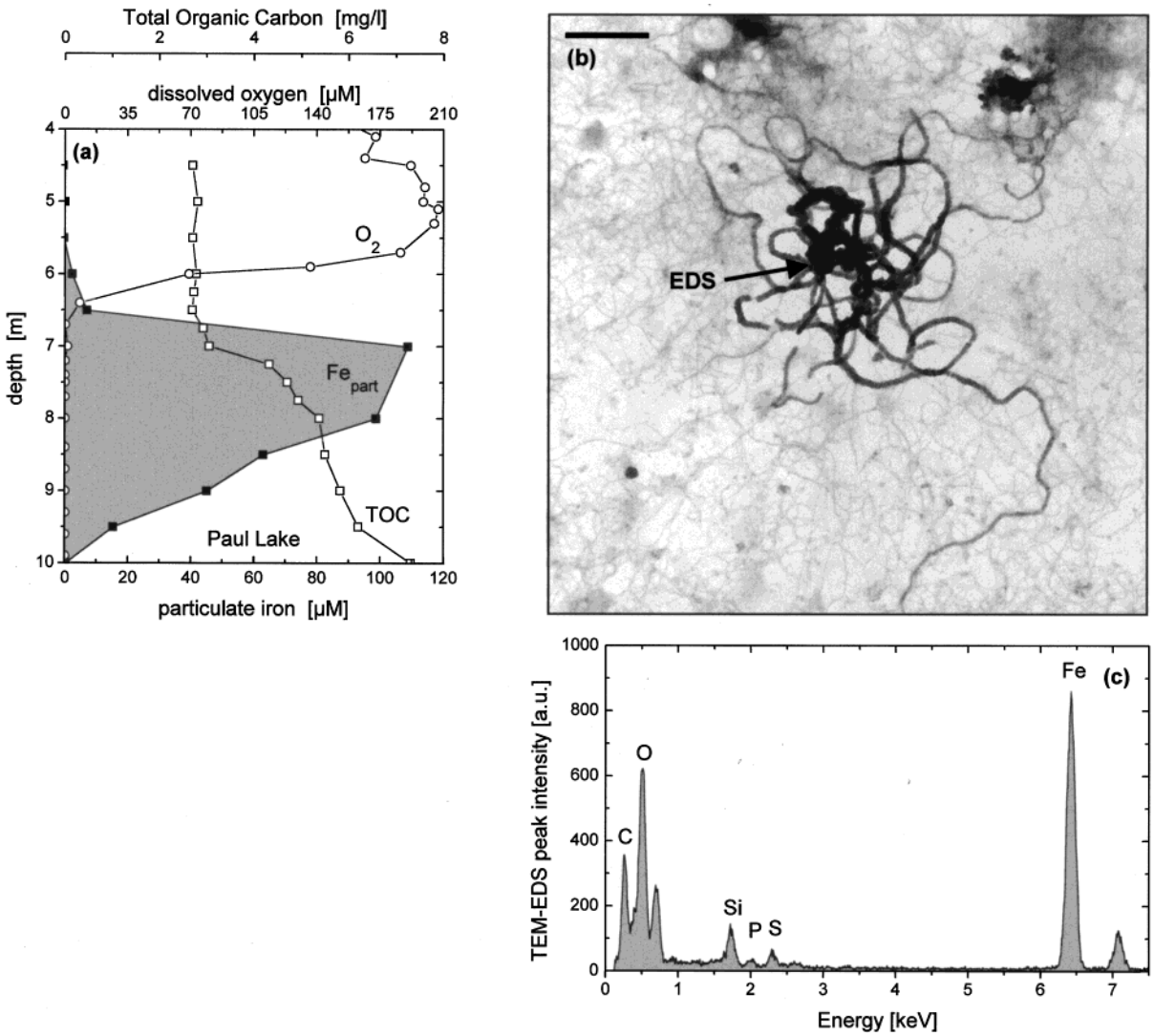

FIGURE 2. (a) Concentration profiles of $[O_2]$, $[Fe]_{part}$ and TOC in the water column of Paul Lake. (b) TEM of typical Fe-rich entities sampled at the maximum of the peak of Fe_{part} (scale bar = 500 nm). (c) Typical elemental analysis (TEM-EDS) of an individual Fe-rich entity.

MNOM and the omnipresence of strong MNOM-Fe interactions.

In the Vallée des Ponts, MNOM has a clear pedogenic origin *(39, 40)*. The conformation of this humic material varies with concentration, pH and ionic strength (I.S.) because of electrostatic effects *(41)*. In our case, a granular humic material, identified in peat samples (Figure 3b,c), acts as nucleation site for the oxidation of Fe(II) when oxic conditions raise from drains to the river. This is confirmed by elemental mapping (STEM-EDS; Figure 3e,f) of the resulting riverine particles which shows a depletion of iron and calcium in their inner core and by electron energy loss spectrometry (TEM-EELS (*29, 39)*) which identifies the core of these particles as carbon-rich.

For lacustrine conditions (aquagenic organic matter), a low $[Fe]_{tot}$:TOC ratio (Lake Lugano) favors the growth of distant Fe-rich nanogranules onto the fibrillar networks (Figure 1b). This process apparently does not modify the morphology of the existing EPS fibrils, which mostly remain attached to the bacteria from which they were produced. A higher $[Fe]_{tot}$:TOC ratio in a low ionic strength medium (Paul Lake) favors coordination of Fe(II) by the chelating groups of MNOM (as compared to other cations), leading to Fe(II)-saturated oxidation/nucleation sites. This coating modifies the structure of MNOM and produces ill-defined Fe-rich entities onto collapsed polysaccharide fibrils (Figure 2b). The systematic association of iron to EPS suggests a template effect of fibrillar organic matter on the formation of the intimate Fe-polysaccharides entities. Similarly, granular humic material (pedogenic organic matter; Vallée des Ponts; Figure 3b) directly favors the oxidation of Fe(II), but the apparently compact structure of the humic material (check the opacity of the organic globules in the peat pore water, Figure 3b) favors the coating of iron-rich material at their surface (Figure 3d). The nature of the dominant organic matter (aquagenic vs pedogenic; flexible vs compact) thus influences the morphology of the resulting Fe-MNOM-rich colloids.

The kinetics of oxidation of Fe(II) are known to be strongly influenced by pH *(15)*, and we expect the fast growing of ill-defined Fe_{part} entities in waters with a high pH. However, when comparing the situation in Lake Lugano ($pH_{Fe-peak} \approx 7.5$) and in Paul Lake ($pH_{Fe-peak} \approx 6.3-6.4$), we observe the opposite: Small granules suggesting slow expansion of Fe_{part} are identified in Lake Lugano, while larger and ill-defined entities are found in Paul Lake. This indicates, in agreement with observations by others (Greifensee, pH = 6.8−7.3) *(42)*, that pH uniquely does not necessarily play a dominant role in the oxidation kinetics of Fe(II) in MNOM-rich waters, as opposed to laboratory syntheses performed under conditions of slow oxidation of Fe(II) solutions in the absence of organic matter.

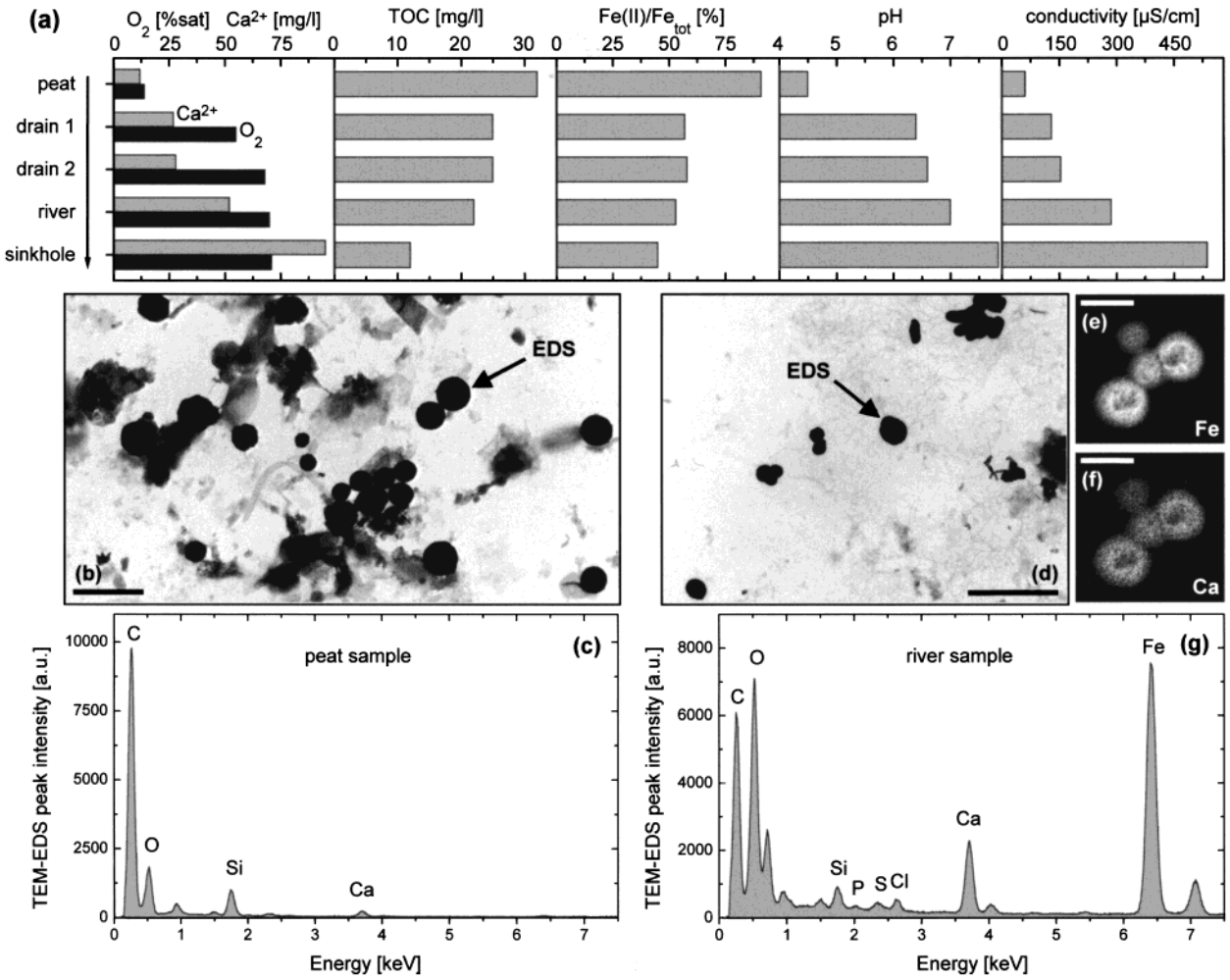

FIGURE 3. (a) Distributions of $[O_2]$, $[Fe(II)]/[Fe]_{tot}$, TOC, pH, conductivity, and $[Ca^{2+}]$ along the drained peat-land area of the Vallée des Ponts. (b) TEM of colloidal organic matter sampled in the peat (scale bar = 1 μm). (c) Typical elemental analysis (TEM-EDS) of an individual C-rich granule in the peat. (d) TEM of typical Fe-rich particles sampled in the Bied River (scale bar = 1 μm); the number concentration of particles in the river as measured by STEM-EDS on individual entities (n = 600) is strongly dominated (>50% of the total number of particles) by Fe-rich globules in the <0.5 μm size range. (e) Elemental map of iron (STEM-EDS) in an assemblage of Fe-rich particles in the river (scale bar = 100 nm). (f) Elemental map of calcium in the same assemblage. (g) Typical elemental analysis of an individual Fe-rich particle in the river.

In the three cases studied, the combination of factors governing Fe_{part} morphotypes is (i) the concentration of total ions, (ii) the relative proportions of $[Fe]_{tot}$ and [NOM], (iii) the nature of the predominant form of MNOM (polysaccharides vs humics), and to a much lesser extent (iv) the pH. Table 1 summarizes these key parameters. Indeed, the interrelation between the different key parameters influencing Fe_{part} is complex and prevents the direct drawing of a unifying quantitative predictive model. The study of aquatic systems presenting other combinations of these key factors should bring further evidences to the aforementioned rules soon.

Differences in the observed morphotypes of Fe-rich particles raise important questions on their transport dynamics through water masses. If one relies on the coagulation theory of hard spheres, the approach of Von Smoluchowski *(43)*, one predicts efficient collisions between submicrometer colloids, leading to larger entities having faster settling velocities *(44)*. Our observations suggest that this process will be strongly hampered for colloids imprisoned in fibrillar networks (Figure 1b, Lake Lugano) which limit the collision efficiency. In addition, highly hydrated polysaccharides will confer a low density to the resulting lacustrine Fe-EPS entities (Figure 1b, Lake Lugano; Figure 2b, Paul Lake), thus reducing their sedimentation rate. Finally, the morphology of Fe_{part} appears to be influenced by hydrodynamic drag forces prevailing in the system *(45)*. This is exemplified by the drop-like morphology of numerous Fe-rich particles identified in the peat-land area (Figure 3d, Bied River), which form under directional hydraulic flow. In this case, the moderate flexibility of MNOM may explain the final shape of particles.

Our results also show that Fe-MNOM-rich particles are far from pure hydrous iron oxides, because they contain nonnegligible to large proportions of other elements. The amount of Si within individual particles is highly variable at each site, but the very constant [P]:[Fe] ratio in the individual Fe-rich microgranules of Lake Lugano (0.48 ± 0.11; $n = 1096$ particles analyzed) indicates the formation of a stoichiometric phase *(33)*, while the fairly constant [Ca]:[Fe] ratio in the Bied River (0.46 ± 0.35; $n = 156$ particles analyzed) suggests a simultaneous entrainment of iron and calcium during the accretion of the humic-rich granules (*39*). The effect of impurities on the chemical reactivity of Fe-rich particles is not well documented *(25)*, and we were not able to highlight the role of foreign ions on the final morphology of Fe-rich particles. Nevertheless, their presence in the matrix of natural Fe-MNOM particles may induce contrasting interactions with trace elements. Consequently, speciation models, which are primarily parametrized for pure iron oxide phases, may not reflect the actual surface reactivity of the realistic Fe-rich morphotypes toward trace elements *(46)*.

TABLE 1: Key Parameters Governing the Morphology of Hydrous Iron Oxides in Lake Lugano, Paul Lake and the Bied River

Key Parameter	Lake Lugano (Fe_{part}-rich layer)	Paul Lake (Fe_{part}-rich layer)	Vallée des Ponts (Bied River after peat)
I.S. [mM]	5	0.4	0.5
$[Fe]_{tot}$ [μM]	< 0.5	100	20
NOM [μM]	100	350	> 1500
nature of NOM	aquagenic EPS	aquagenic EPS	pedogenic humics
$[Fe]_{tot}$:[NOM] ratio	$< 5\times10^{-3}$	*ca.* 0.3	$< 10^{-2}$
pH	≈ 7.5	≈ 6.5	≈ 7
Relative influence of key parameters	high I.S. *vs.* low $[Fe]_{tot}$: major ions compete with Fe(II) for complexation by NOM, leaving distant anchors for Fe(II); low $[Fe]_{tot}$:[NOM] favours the formation of granules; high pH may slightly increase the oxidation rate	low I.S. *vs.* high $[Fe]_{tot}$: high density of anchor sites available on NOM for Fe(II) complexation, resulting in Fe(II)-overloaded NOM; high $[Fe]_{tot}$:[NOM] favours heavily loaded entities; lower pH may slightly decrease the oxidation rate	Low I.S. *vs.* moderate $[Fe]_{tot}$: high density of anchor sites available on NOM for Fe(II) complexation, leading to Fe(II)-loaded NOM; Very low $[Fe]_{tot}$:[NOM] favours poorly loaded entities; pH has no strong influence on the oxidation rate
Resulting Fe_{part} morphotype	10-50 nm granules attached to EPS networks 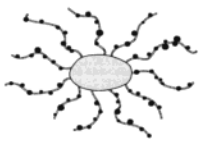	Ill-defined Fe-EPS intimate mixtures 	100-500 nm spherical and drop-like globules with C-rich core 

To conclude, we have shown that in various environmental settings hydrous iron oxides systematically present specific morphotypes that are always associated with natural organic matter. Different types of MNOM and water compositions exert different effects on the production of the hydrous iron oxides. These iron oxides can contain an important proportion of foreign ions. Our observations allow us to propose a general and simple scheme to predict the most probable Fe-rich morphotype that should be identified in a water body of known composition (see Table 1).

The important scavenging property of Fe-MNOM entities toward foreign ions, in turn, is likely to affect the nominal reactivity of the iron oxides. This information is only accessible through the careful investigation of particles at the microscopic level accompanied by modern analytical methods (TEM-EDS, TEM-EELS) probing their elemental composition. It is clear that the morphology of the material should influence their transport behavior, while their chemical composition should modify their reactivity. For these reasons, our observations open new opportunities for understanding the role of iron particles in the scavenging of trace elements under natural conditions.

Acknowledgments

This is a contribution to the University of Lausanne (Institute of Inorganic and Analytical Chemistry), Northwestern University (Department of Civil Engineering), the University of Geneva (F.-A. Forel Institute), the University of Neuchâtel (Center of Hydrogeology), and the University of Notre Dame (Environmental Research Center). Thanks are due to M. Taillefert, C.-P. Lienemann, D. Mavrocordatos, C. Mondi and M. Monnerat for sampling and analyses, and to three anonymous reviewers for helpful comments and improvement of the manuscript. Financial contributions were provided by the Swiss National Science Foundation through Grants #: 20-42250.94, 50-39145.93, 20-33569.92, and 21-43438.95; and the U.S. National Science Foundation through Grants # EAR-9815090 and BES-9596252.

Literature Cited

(1) Einsele, W. *Arch. Hydrobiol. Plankt.* **1937**, *33*, 361.
(2) Mortimer, C. H. *J. Ecol.* **1941**, *29*, 280; **1942**, *30*, 147.
(3) Salomons, W.; Förstner, U. *Metals in the Hydrocycle*; Springer: Berlin, 1984.
(4) Sigg, L. In *Chemical Processes in Lakes*; Stumm, W., Ed.; Wiley: New York, 1985; p 283.
(5) Sigg, L. In *Aquatic Surface Chemistry*; Stumm, W., Ed.; Wiley: New York, 1987; p 319.
(6) Honeyman, B. D.; Santschi, P. H. In *Environmental Particles I*; Buffle, J., van Leeuwen, H. P., Eds.; Lewis: Chelsea, 1992; p 379.
(7) Schindler, P. W.; Stumm, W. In *Aquatic Surface Chemistry*; Stumm, W., Ed.; Wiley: New York, 1987; p 83.
(8) Capel, P. D.; Eisenreich, S. J. *J. Great Lakes Res.* **1990**, *16*, 245.
(9) Riise, G. *Sci. Tot. Environ.* **1994**, *152*, 91.
(10) Buffle, J.; Perret, D.; Newman, M. In *Environmental Particles I*; Buffle, J., van Leeuwen, H. P., Eds.; Lewis: Chelsea, 1992; p 171.
(11) Dzomback, D. A.; Morel, F. M. M. *Surface Complexation Modelling: Hydrous Ferric Oxide*; Wiley: New York, 1994.
(12) Westall, J. C. In *Aquatic Surface Chemistry*; Stumm, W., Ed.; Wiley: New York, 1987; p 3.

(13) Stumm, W. In *Aquatic Chemistry: Interfacial and Interspecies Processes*; Huang, C. P., O'Melia, C. R., Morgan, J. J., Eds.; ACS: New York, 1995; p 1.
(14) Schneider, W.; Schwyn, B. In *Aquatic Surface Chemistry*; Stumm, W., Ed.; Wiley: New York, 1987; p 167.
(15) Davison, W.; DeVitre, R. R. In *Environmental Particles I*; Buffle, J., van Leeuwen, H. P., Eds.; Lewis: Chelsea, 1992; p 315.
(16) Leppard, G. G.; Buffle, J.; DeVitre, R. R.; Perret, D. *Arch. Hydrobiol.* **1988**, *113*, 405.
(17) Leppard, G. G.; DeVitre, R. R.; Perret, D.; Buffle, J. *Sci. Tot. Environ*. **1989**, *87/88*, 345.
(18) Buffle, J.; DeVitre, R. R.; Perret, D.; Leppard, G. G. *Geochim. Cosmochim. Acta* **1989**, *53*, 399
(19) Fortin, D.; Leppard, G. G.; Tessier, A. *Geochim. Cosmochim. Acta* **1993**, *57*, 4391.
(20) Tessier, A.; Belzile, N.; DeVitre, R. R.; Leppard, G. G. *Geochim. Cosmochim. Acta* **1996**, *60*, 387.
(21) Tiller, C. L.; O'Melia, C. R. *Colloids Surf. A* **1993**, *73*, 89.
(22) Wilkinson, K. J.; Stoll, S.; Buffle, J. *Fresenius J. Anal. Chem*. **1995**, *351*, 54.
(23) Wehrli, B. In *Aquatic Chemical Kinetics*; Stumm, W., Ed.; Wiley: New York, 1990; p 311.
(24) Buerge, I. J.; Hug, S. J. *Environ. Sci. Technol.* **1998**, *32*, 2092.
(25) Cornell, R. M.; Schwertmann, U. *The Iron Oxides*; VCH: Weinheim, 1996.
(26) Hofmann, A. Dr. Thesis, University of Geneva, Switzerland, 1996.
(27) Lienemann, C.-P. Dr. Thesis, University of Lausanne, Switzerland, 1997.
(28) Taillefert, M. Ph.D. Thesis, Northwestern University, U.S.A., 1997.
(29) Mavrocordatos, D. Dr. Thesis, University of Lausanne, Switzerland, 1997.
(30) Mondi-Couture, C. Dr. Thesis, University of Lausanne, Switzerland, 1999.
(31) Lienemann, C.-P.; Taillefert, M.; Perret, D.; Gaillard, J.-F. *Geochim. Cosmochim. Acta* **1997**, *61*, 1437.
(32) Lienemann, C.-P.; Heissenberger, A.; Leppard, G. G.; Perret, D. *Aquat. Microb. Ecol.* **1998**, *14*, 205.
(33) Lienemann, C.-P.; Monnerat, M.; Dominik, J.; Perret, D. *Aquat. Sci.* **1999**, *61*, 133.
(34) Taillefert, M.; Lienemann, C.-P.; Gaillard, J.-F.; Perret, D. *Geochim. Cosmochim. Acta* **2000**, *64*, 169.
(35) Atteia, O.; Perret, D.; Adatte, T.; Kozel, R.; Rossi, P. *Environ. Geol.* **1998**, *34*, 257.
(36) Perret, D.; Leppard, G. G.; Müller, M.; Belzile, N.; DeVitre, R. R.; Buffle, J. *Aquat. Sci.* **1991**, *25*, 1333.
(37) Thiéry, J.-P. *J. Microsc. (Paris)* **1967**, *6*, 987.
(38) Chenu, C. *Geoderma* **1993**, *56*, 143.
(39) Couture, C.; Mavrocordatos, D.; Atteia, O.; Perret, D. *Phys. Chem. Earth* **1998**, *23*, 153.
(40) Bouyer, Y.; Kübler, B. *J. Hydrol.* **1981**, *54*, 315.
(41) Ghosh, K.; Schnitzer, M. *Soil Sci.* **1980**, *129*, 266.
(42) Emmenegger, L.; King, D. W.; Sigg, L.; Sulzberger, B. *Environ. Sci. Technol.* **1998**, *32*, 2990.
(43) Von Smoluchowski, M. Z. *Phys. Chem*. **1917**, *92*, 129.
(44) Hirtzel, C. S.; Rajagopalan, R. *Colloidal Phenomena, Advanced Topics*; Noyes, Park Ridge, 1985.
(45) van Leeuwen, H. P. In *Environmental Particles I*; Buffle, J., van Leeuwen, H. P., Eds.; Lewis: Chelsea, 1992; p 497.
(46) Taillefert, M.; Rose, E.; Gaillard, J.-F. In *Proceeding for the 3rd International Conference on the Biogeochemistry of Trace Elements*; Prost, R., Ed.; INRA-Publications: Versailles, 1995; p 289.

Received for review January 6, 2000. Revised manuscript received May 23, 2000. Accepted June 15, 2000.

ES0000089